Maastricht University

PRA3002 Lab Report 1

O1 – Interference and Diffraction of Light [Double Slit Experiment]

Maastricht Science Programme

2024-2025

Author:

Nils Thiessen

Team members:

Konstantinos Ioannou, Miguel Miralda, Nils Thiessen

Instructors:

Chris Pawley, Sanne Aarts

15th November 2024

Contents

1 Introduction

In the duration of this lab, the wave-like behaviour of light will be explored through analysis of the different interference patterns in a single and double slit experiment. The aim is to observe the effect of differing slit widths and distances in between. By applying the theory underlying the experiments, an attempt will be made at deducing these slit properties.

Comprehending the nature of light has long been a topic of discussion for scientists. One point of conflict underlying these debates was whether it belonged to the category of particles or that of waves. One idea prevalent during the 17th and 18th century, further expanded by Isaac Newton, revolved around light being a flux of particles (or corpuscles, as they were called) [1]. However, a rather simple experiment introduced by Thomas Young in his paper *On the theory of light and colour* published in 1801 supposedly contradicted that notion. By passing a beam of light through singular and double slits and observing the interference pattern projected on a screen, one could clearly infer that the source thereof must have acted wave-like. [2]

Though many people could not abandon Newton's theory yet, the dual nature of light as both particle (i.e. photons) and waves (electromagnetic radiation, that is) is widely known nowadays [1]. The experiment became the foundation for modern quantum mechanics. Furthermore, variations in the setup like the implementation of electrons as a source lead to important discoveries, such as the general wave-particle duality of quantum objects. [3]

1.1 Theory

Though being massless, photons carry intrinsic energy with them. The extend thereof determines the frequency f at which the fields oscillate, according to Equation 1. [4]

$$E = hf \tag{1}$$

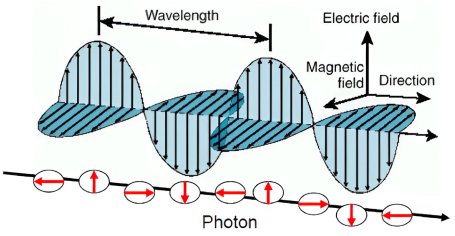

Figure 1: Vector of electric and magnetic field of a photon as it propagates through vacuum. [4]

h is known as the Planck's constant. Being a wave propagating at vacuum speed c, one can describe the relation between its wavelength λ and frequency f as: [4]

$$c = \lambda f \tag{2}$$

1.1.1 General Setup

The idea behind the slit experiments is something that can be replicated with other types of waves. A coherent wave arrives at a boundary with an opening of certain width, and is thus diffracted in that it spreads out afterwards.

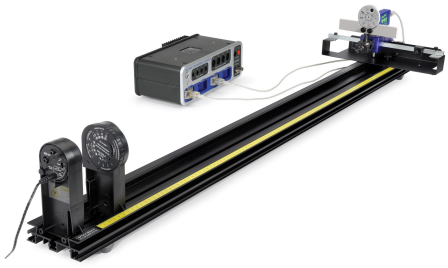

Figure 2: Experimental Setup for the Diffraction of Light Experiment. For size comparison: Length of optics track is roughly 1.2 m. [5]

In this example, the experiment consists of a laser on one end of a trail pointing at a screen on the other end. A barrier blocking the beam everywhere except at one or multiple slits is put in between. Upon inserting these diffraction slits, an interference pattern appears on the screen. When measuring the light intensity along the direction of the pattern, it can be quickly seen that each peak is separated to its neighbour by a similar distance. The exact type of pattern is correlated to the number of slits, the distance between them and the wavelength of the incoming particles.

1.1.2 Lasers

Photons are produced in a variety of electromagnetic processes. In nature, the creation of photons often occurs as a byproduct of particles undergoing transitions. Simply stated, a part of the energy underlying them is put into the emission of photons. [6]

Naturally, the ideal situation for experimentalists would be a device emitting a uniform, focused beam. However, these particles, when derived from light sources, can be found in a spectrum of wavelengths (and thus frequencies) akin to the energy lost in the corresponding processes of their creation. The Sun generates photons with a broad spectrum [7]. This is which well visualized when passing through refractive media, where the refraction differs according to the particle's wavelength. Additionally, the photons are usually not radiated directionally, while wave-like properties such as their phase vary.

Light beams created by lasers do not exhibit these characteristics. Rather, they are coherent - no differentiation between direction and time of each particle wave - and monochromatic. Key to this behaviour is their composition and the underlying mechanisms. Electrons in the atoms contained in these devices are found in a specific metastable state, with a specific energy difference ΔE to the ground state [8]. Photons with energies equal to ΔE are shot through this medium and in a mechanism called *stimulated emission*, some electrons de-excite and radiate photons with same properties, causing a chain reaction. [8]

As a result, the outgoing beam will act as one wave front.

1.1.3 Single Slit Experiment - Underlying Concepts

The incident wave coming from the laser can be viewed as a wavefront. After passing through the slit, in line with Huygen's principle one can also view the wave as a superposition of smaller wavelets, derived from any point along the front. each part of the wave as a single wavelet. Literally, the once homogeneous beam of in-phase photons is now split up into the individual components. [9]

The screen is positioned a distance D away from the boundary. For later purposes, it is necessary to clarify that the value of D is far larger than the slit's width a. Although the photons start out in-phase, their path until they arrive at a common destination differs, most importantly in its length. Every point, when zooming out from the quantum level, will be hit by several rays.

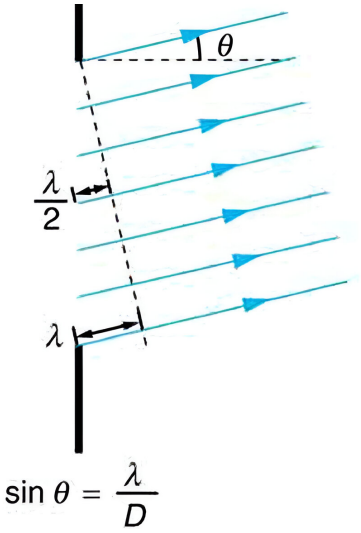

Figure 3: Visualization of different particle tracks upon diffraction at the single slit, on trajectory to the first minimum at an angle θ to the optical axis. The path difference δ between the tracks commencing at each end of the slit is λ. [9]

One can define the optical axis as the line that would be traced as a continuation of the incident beam, with the photon's wavelength λ. Under the condition $D \gg a$, the paths from any point on the slit to the common destination can be approximated to be at the same angle θ to this optical axis. These waves will now be out-of-phase. [9]

However, at specific points on the screen, destructive interference occurs (corresponding to minimum intensities). Any ray (e.g. from the edge) has to be $\frac{\lambda}{2}$ out-of-phase from another one (e.g. the center), or multiples thereof. In other words, the path difference has to be $\delta = l' - l$. As can be seen in Figure 3, the angle θ_{min} for the m^{th} minimum can be found in Equation 3:

$$a \sin[\theta_{min}] = m\lambda \tag{3}$$

m can take all integer values besides 0, which would imply $\theta = 0$. At that angle, all rays arrive in-phase, due to their path length staying the same. Decreasing the slit width a means increasing the angular increments between consecutive minima. [5]

The nature of interference between the rays causes the central maximum at $\theta = 0$ to be far bigger than the ones left and right to it.

1.1.4 Double Slit Experiment - Underlying Concepts

Adding another slit **B** a distance d from slit **A** leads to further complexities. The pattern observed on the screen is influenced by the interference between waves from **A** and **B**. Constructive interference occurs when these arrive (on average) in-phase, while destructive interference does so during out-of-phase waves. The path length difference for constructive interference can thus be found using Equation 4:

$$d\,sin\,[\varphi_{max}] = n\lambda \tag{4}$$

Here, n represents the n^{th} maximum from the central one. The parameter can take integer values including 0. The intensity measured on the projection surface is now affected by the theory behind both Equation 3 and Equation 4, with d normally being larger than a. Mathematically, it becomes obvious then that the angular separation between consecutive peaks, as induced by 4, has to be rather small to compensate the size of d. In comparison, the minima calculated from 3 will be larger in scale.

1.2 Hypothesis

The lab session discussed in this report will replicate Young's setup, consisting of two parts. In the single slit experiment, the variation of the pattern under changes in the slit width will be observed. It is to be expected that larger slit widths result in smaller angular separation, and thus peaks closer to each other. Furthermore, it will be attempted to discern the slit widths from the pattern alone. However, some complications in the value's accuracy will most likely occur, considering the scale of the distances concerned.

The double slit experiment will center around the patterns caused by both different slit widths and distance between them. From theory, one should find that the effect of the slit widths can be seen in the large-scale fluctuations, like those found in the single slit experiment, while a higher distance should decrease the separation between consecutive peaks. It can be estimated that an endeavour at deducing the distance between the slits will suffer to the same constraints as in the first experiment.

2 Materials & Methods

2.1 Setup

The materials used for the experiment are included in the PASCO product EX-5545A ([5]).

The setup was built as visualized in Figure 2. The red laser diode, with a wavelength $\lambda = 650nm$, was placed at one end of an optics track facing the other side. A rotatable precision diffraction slit corresponding to the desired number of slits was mounted in front of it. Secured at the other end, the combination of Rotatory Motion Sensor and Linear Translator allowed the attachment of a Light Sensor thereon over a rod. The Light Sensor Setup provided additional features, mainly the projection display merged with an aperture slit disk.

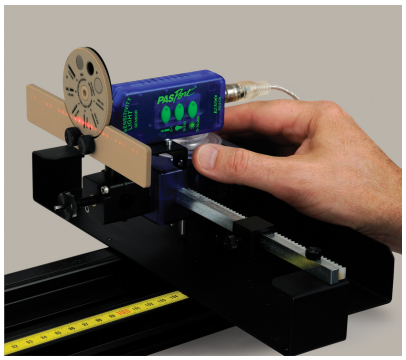

Figure 4: Light Sensor Setup: An interference pattern can be seen on the projection display, at the same level as the aperture slit. [5]

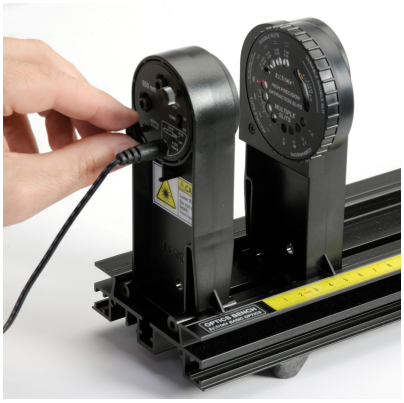

Figure 5: Diffraction Laser Setup: Adjusting the knobs changes the vertical and horizontal placement of the laser. [5]

As can be seen in Figure 4, activating the laser under proper safety considerations resulted in an interference pattern. For optimal placement and intensity, one could adjust the knobs on the laser diode shown in Figure 5 for horizontal and vertical placement, until a strong signal was displayed on top of the aperture slit.

The distance between the slit disk and the light sensor came down to $(D = 0.943 \pm 0.01)m$, as derived from a meter stick. The error arises from the inaccuracy in precisely determining the positions of both ends. Compared to the slid width a and the normal separation between slits d (at the order of $10^{-4}m$), one can safely state that $D \gg a, d$ and apply the theory.

The Light and Rotatory Motion Sensor were connected to PASCO Capstone, with data logging at a frequency of 50 Hz. During the data capturing process, the setup was moved from left to right, such that the Light Sensor could measure the light intensity at each point along the pattern. Changing the position more slowly would yield more accurate data. In Capstone, one could then create figures plotting relative intensity against position. Three buttons at the side of the Light Sensor were responsible for modify the sensitivity of measurement. In general, higher

intensities required less sensitive logging, potentially ending in inaccurate measurements.

2.2 Single Slit - Finding the slit's width *a*

During the first part of the lab session, measurements were taken based on single slits of distinct widths, implementing the rotatable disk with single slits apertures. For $a = (0.02 \pm 0.005)mm$, the sensitivity mode of the Light Sensor stayed at maximum sensitivity, namely the 0-1 button. For $a = (0.04 \pm 0.005)mm$, $a = (0.08 \pm 0.005)mm$ and $a = (0.16 \pm 0.005)mm$, higher intensities required the 0-100 mode. Although several options for the aperture were tested, the 1mm slit aperture was chosen for the single slit analysis conducted in this paper.

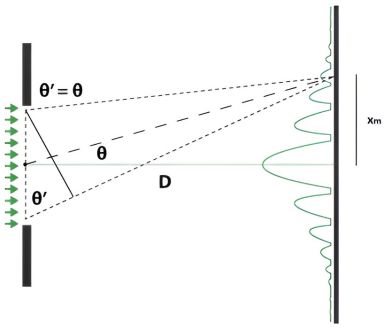

Figure 6: Visualization of different paths towards the common destination: From the triangle formed by the displacement x_m from the maximum and the distance between screen and slit, one can replace the angle. [10]

Although the angle θ cannot be directly measured, one can infer it from trigonometric rules portrayed in Figure 6. Due to the large distance D between screen and slits, small angle approximation applies, with $sin[\theta] \approx tan[\theta]$. From the corresponding triangle:

$$tan[\theta] = \frac{x_m}{D} \tag{5}$$

Equation 5 includes the distance x_m between central maximum and a point on one side of it. To improve on the accuracy, the measurement was conducted from a considerable number of minima to the right until the same number of minima to the left of the peak, yielding $\Delta x = 2x_m$. Equation 5 is then modified to account for the specific measurement:

$$tan[\theta] = \frac{\Delta x}{2D} \tag{6}$$

Ultimately, adjusting Equation 3, the slit width can be calculated as seen below.

$$a = \frac{m\lambda}{sin[\theta]} \approx \frac{2D\lambda}{\Delta x}m \tag{7}$$

2.3 Double Slit - Finding the slit separation *d*

In order to conduct measurements for the second part of the lab session, the boundary in front of the laser was replaced by a rotatable disk with double slits of distinct slit sizes. Although data

was taken with several variations, the analysis performed in this paper relies on the constant slit width $a = (0.04)mm$, so that the peaks around the central maximum had a considerable width. The aperture disk setting used was a slit aperture of 0.5mm, ensuring that each peak could be properly distinguished from the rest, avoiding one to be swallowed by the background noise. The separation d between the slits was varied between $d = (0.25 \pm 0.005)mm$ and $d = (0.5 \pm 0.005)mm$.

The conditions in deriving Equation 6 still apply, while Δx represents the distance between points number of maxima to the right and to the left of the central maximum. d can therefore be calculated with:

$$d = \frac{n\lambda}{sin[\varphi]} \approx \frac{2D\lambda}{\Delta x}n \tag{8}$$

3 Results & Analysis

3.1 Single Slit: Results

For each single slit width, the intensity along the interference pattern was measured and plotted against position as discussed in Section 2.2. Worthy of note is that the value for the actual sizes was only known with an uncertainty of ±0.005mm. Figure 7a) portrays the intensity-position graph resulting from diffraction through an $a = 0.02mm$ slit. The aim was to locate a minimum on the left and on the right of the central maximum. However, for this specific data, one cannot assume these positions with absolute certainty, since the spread is too large. As such, calculations to find experimental values for $a = 0.02mm$ are redundant.

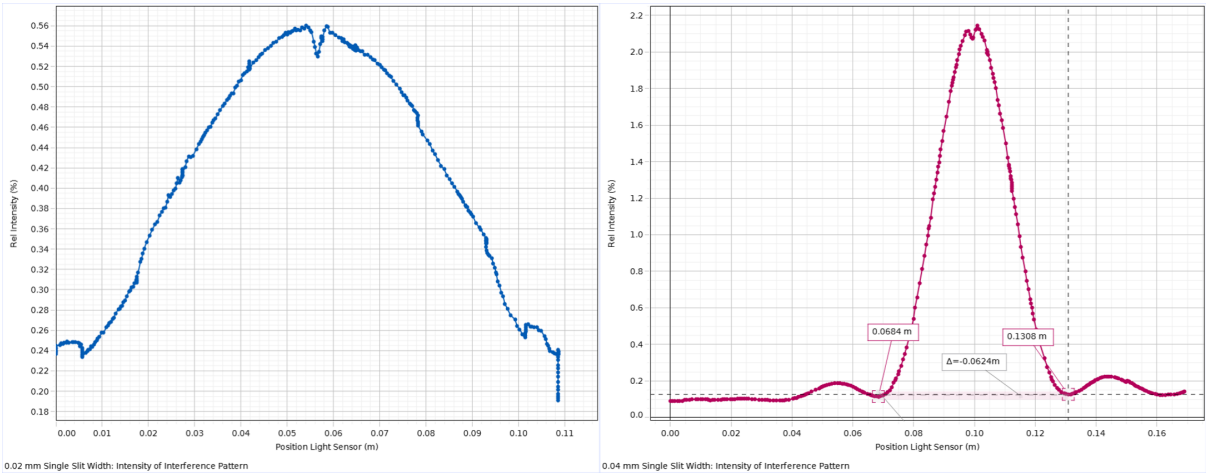

Figure 7: Intensity vs Position plots. In a), for $a = 0.02mm$, finding minima is not possible with high precision, since the data mainly consists of the central peak. In b), for $a = 0.04mm$, two minima are located, while the change in position is calculated with the Delta tool. One can observe a smaller spread than in a).

The story is different for Figure 7b). Two minima are located to the left and right of the central maximum, with the distance between them corresponding to the separation between two minima ($m = 2$). Although these values represent the lowest recorded point in the corresponding valley, the actual minimum might as well be located between the data points left and right of it. The movement of the light sensor did not occur at a constant rate. As such, for an individual uncertainty accompanies each recorded point.

One important conclusion made by observing the graphs is that the spread across the projection surface becomes smaller. For higher slit widths, one can observe minima at smaller distances to the central axis. In addition to that, the central maximum has a far higher intensity than its neighbouring peaks. This phenomenon is even more prevalent in Figure 8:

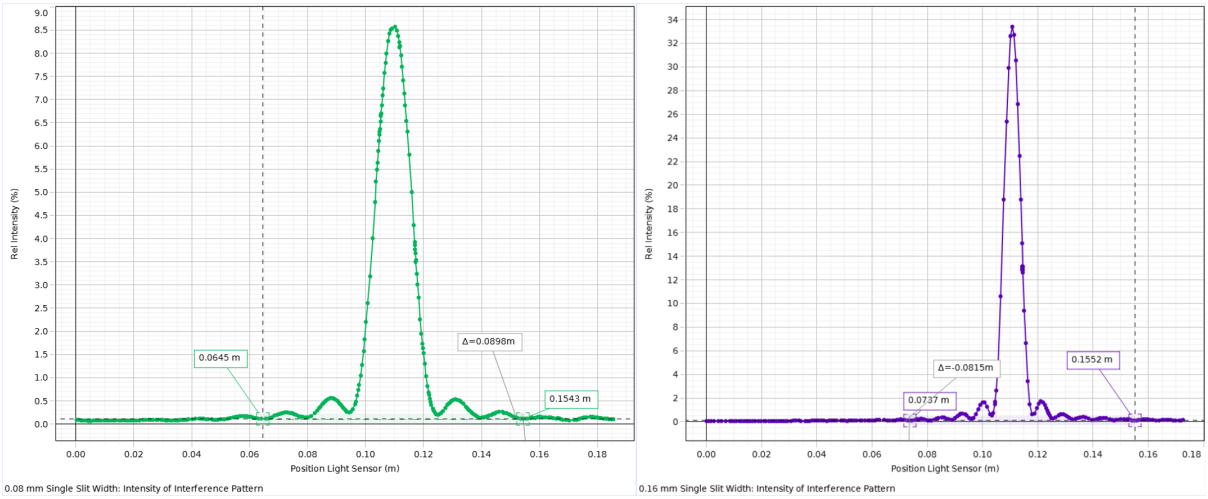

Figure 8: Intensity vs Position plots. In a), for $a = 0.08mm$, and b), for $a = 0.16mm$, two minima are located, while the change in position is calculated with the Delta tool. One can observe a smaller spread for larger a.

For each slit width the positions and distance Δx were documented, with the corresponding error $\varepsilon_{\Delta x}$. The calculation of the experimental value for a is dependent on the distance between screen and slit D, for which the measurement error was already given as $\varepsilon_D = 0.01m$. Assuming that the outcome was not influenced by any other major uncertainties (the wavelength of the laser is quite precise), one can use error propagation to find the total error in a:

$$\Delta a_{exp} = a_{exp}\sqrt{(\frac{\varepsilon_{\Delta x}}{\Delta x})^2 + (\frac{\varepsilon_D}{D})^2} \tag{9}$$

Ultimately compiling the information in Table 1:

a_{theory} [mm]	Left minimum [m]	Right minimum [m]	Distance between points Δx [m]	Number of minima m	a_{exp} [mm]
0.02 ± 0.005	-	-	-	-	-
0.04 ± 0.005	0.0684 ± 0.0007	0.1308 ± 0.0008	0.0624 ± 0.0015	2	0.03929 ± 0.00103
0.08 ± 0.005	0.0645 ± 0.001	0.1543 ± 0.0009	0.0894 ± 0.0019	6	0.08228 ± 0.001954
0.16 ± 0.005	0.0737 ± 0.001	0.1552 ± 0.0008	0.0815 ± 0.0018	11	0.16546 ± 0.00405

Table 1: Comparison between theoretical slit width a and experimental one. A minimum left and one right to the central maximum are located, with the distance between them corresponding to the number of minima m. The experimental value is then calculated using Equation 7.

3.2 Double Slit: Results

A similar procedure was conducted for the double slit experiment, with the slit width fixed at $a = 0.04mm$. Plotting the intensity along the interference pattern due to the slit separations $d = 0.25mm$ and $d = 0.5mm$, Figures 9a) and Figure 9b) appear.

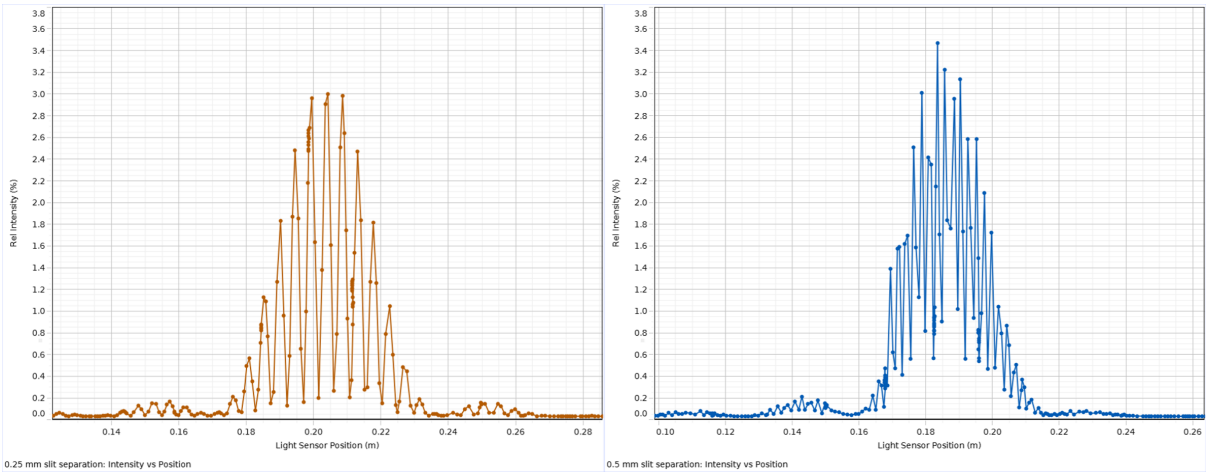

Figure 9: Intensity vs Position plots at fixed slit widths $a = 0.04mm$. In a), for $d = 0.25mm$, and b), for $d = 0.5mm$, two maxima inside the central envelope are located, used for calculation of the separation between them. One can observe more peaks packed into the envelope for larger d.

A few observations about the shape of the graphs are noteworthy. To begin with, although small term fluctuations depend on d, there is no change in the overall shape of the graph. It appears that the interference pattern caused by a single slit of $a = 0.04mm$, as seen in Figure 9b), acts as an envelope under which the intensity oscillates.

Furthermore, by increasing the slit separation d, the distance between consecutive peaks becomes smaller. Not only that, but whole peaks might also be swallowed in the process of moving the light sensor. Note that for both Sections 3.1 and 3.2, data logging by the Rotatory Motion Sensor is precise enough to ignore the resulting inaccuracy. While the for the separation between maxima $\varepsilon_{\Delta x}$ will still be calculated as outlined in Section 3.1, the whole data might be affected by missing peaks.

Due to similar formulas, the propagation of error occurs similar to that of the slid width:

$$\Delta d_{exp} = d_{exp}\sqrt{(\frac{\varepsilon_{\Delta x}}{\Delta x})^2 + (\frac{\varepsilon_D}{D})^2} \tag{10}$$

Collecting the result in Table 2:

d_{theory} [mm]	Left minimum [m]	Right minimum [m]	Distance between points Δx [m]	Number of maxima n	d_{exp} [mm]
0.250 ± 0.005	0.1852 ± 0.0015	0.2226 ± 0.0020	0.0374 ± 0.0035	8	0.26222 ± 0.02470
0.500 ± 0.005	0.1694 ± 0.0013	0.2018 ± 0.0019	0.0324 ± 0.0032	14	0.52971 ± 0.05262

Table 2: Comparison between theoretical slit separation *d* and experimental one. A maximum left and one right to the central maximum are located, with the distance between them corresponding to number of maxima n. The experimental value is then calculated using Equation 8.

3.3 Overview Results

The percentage deviation of the experimental value from the theoretical one can be calculated using $\left(\frac{V_{exp}-V}{V}\right) \times 100$, where V corresponds to the value.

Assembling the theoretical and experimentally determined values from Tables 1 and 2 into one collection:

	Theory Value [mm]	Experimental Value [mm]	Percentage Deviation [%]
a	0.04	0.03929	-1.775
	0.08	0.08228	2.850
	0.16	0.16546	3.413
d	0.25	0.26222	4.888
	0.50	0.52971	5.942

Table 3: Compiling Tables 1 and 2: Experimentally determined values vs their theoretical one, along with their deviation from one another.

4 Discussion

During the experiment, the effect of varying the slit width a for single and slit separation d for the double slit experiment were analyzed. It was observed if one could accurately determine a and d by inspecting the interference pattern projected onto the display. In Section 1.1, several predictions were made as to which shapes these patterns would take and the accuracy of the established experimental values.

4.0.1 Single Slit - Discussion

Figures 7 and 8 portray how the slit width affects the shape of the pattern. Generally, a bigger value for a implied a narrower spread, such that the separation between consecutive peaks decreased. Equation 3 from Section 1.1.3 describes exactly this behaviour. For a specific minimum n, the angle has to compensate for changes in a. The angular increments, affecting the separation between consecutive peaks, needs to be smaller for higher values of a.

An obvious remark has to be made about the abnormal intensity of the central maximum in contrast to any surrounding one. However, this is in line with Section 1.1.3. At each point on the screen, photons in different phases arrive. For the points in the direction of the original beam, they are only hit by waves that are in-phase, so the interference is largely constructive. Moreover, at larger angles θ, less rays reach a common destination. For $\theta \approx 0$, that is at the central maximum, the described effect barely applies.

The experimental values a_{exp} for the slit widths deviate little from the actual values. When accounting for the uncertainty about the actual slit size as well as the error for the experimental result calculated in 9, the values align for $a = 0.04mm$, $a = 0.08mm$ and $a = 0.16mm$. Nonetheless, there is a general increase in the percentage deviation until $a = 0.16mm$. One could explain the finding by noting that the smaller sizes of the minima, caused by the bigger slit width, provides bigger room for estimating the positions incorrectly. Additionally, the minima chosen are farther away from the central axis. The whole analysis relied on the condition of θ being rather small, with $D \gg a, x_m$. The formulas derived might not be applicable in this particular case.

4.0.2 Single Slit - Discussion

Figure 9 shows how the intensity-position graph differs depending on the slit separation d, which especially affects the short-term fluctuations. An increasing slit separation appears to lead to smaller distances between consecutive peaks, which is theoretically supported by

Equation 4. For $a = 0.04mm$, the similarity of the single and double slit interference pattern is remarkable, with the width of the single apparently deciding the general shape thereof. Without this limitation, the intensity would oscillate at the same amplitude, which would violate the conservation of energy.

The percentage deviation between the experimental and theoretical value of d (4.888 and 5.942) are rather large. However, the errors in d_{theory} and d_{exp} can explain the deviation of one another quite well.

4.1 Improvement on Uncertainties

The biggest contributor to the uncertainties, especially for smaller slit widths, can be found in the precision values for theoretical a and d, which were given as ±0.005mm. Even for $a = 0.16mm$, this corresponds to an uncertainty of 3.125%. Although larger slits would narrow the described possible alteration, the resulting patterns would be neither ideal nor comparable. Changing the laser's wavelength might do the trick, but not while the photons stay in the visible light spectrum. It appears that the simplest way is to use slits with lower precision values.

Although the contribution is comparably small, there are smarter ways to evaluate the distance D between the Light Sensor and the slits. As an example, one could move a motion sensor along the track until it (or whatever is attached to it) hits both devices.

The uncertainty in Δx is more laborious to fix. Normally, measuring several peaks and averaging them would simply reduce the error. However, the caveat coming along with it is that the condition of small θ would be quickly nullified, possible worsening the result.

Although the sampling frequency of the devices was already set at 50 Hz, increasing it could also be an option. However, the main issue would lie in the inconsistency in changing the position of the Light Sensor. In the described setup, the disk responsible for the motion sensors movement was rotated by hand, leading to abrupt changes. The apparatus could be improved by automizing this process. The disk could be rotated over a string, which could additionally be attached to another motion sensor revolving at a constant rate.

The aperture slits in front of the Light Sensor had a width of 0.5mm and 1mm. At lower widths, the general amplitude of the graphs decreased, hence these apertures were decided upon. That being said, the smaller amplitude could also be used to the experimenter's advantage, as the most sensitive mode of the Light Sensor would be applicable for these measurements, leading to more accurate readings.

4.2 Further experiment

The general alignment between experimental and theoretical values promises potential for further experiments conducted with the applied setup, apart from those already discussed in Section 4.1.

One idea is to change the wavelength of the laser inside the visible light spectrum. This alteration would not only impact the colour of projected pattern, but also the separation between consecutive peaks. The results could be compared to theory, or it could even be tried to calculate the wavelength from the results alone. However, the uncertainties in slit sizes do not bode well for the latter.

So far, only single and double slit diffraction has been considered. Adding more slits will complicate the resulting pattern, but one should be able to account for that in calculations. Hence, the patterns caused by a differing number of slits with consistent widths and separations might be educational.

The setup utilized or even the type of experiment is not unique to lasers and light. Any type of wave will, under the correct setup apt for the wavelength, induce a similar interference pattern. Not only that, but alike experiments have also been done with other particles, including electrons and neutrons. A comparison between them might lead to interesting conclusions.

Generally, the focus of this lab session has neglected the aperture sizes in front of the Light Sensor. Depending on the sizes, the interference pattern might not appear at all. Varying the apertures and analyzing the impact on the intensities could have real applications. This lab could thus lead to more practical considerations. [11]

5 Conclusion

The lab session aimed at analyzing the interference pattern caused by changing the slit widths a and separations d for the single and double slit experiment, in the hopes of calculating values for a and d in line with those suggested by theory.

It can be generally stated that the goals have been met, with the maxima and minima in the interference patterns appearing at the angles supported by Equations 3 and 4. It was noted that the intensity graph caused by a single slit acted as an envelope for the double slit intensity graphs, with the slit separations causing short-term fluctuations beneath.

The experimentally determined values for both a and d matched the theoretical ones quite well, with the highest percentage deviation being 5.942 %. The deviations could be explained by the uncertainties, caused by both the large imprecision on the theoretical side and the methodology on the experimental side. As such, various suggestions have been brought forward in Section 4.1 to tackle these problems, ranging from replacing the slits with higher precision ones to ensuring a more uniform, steady change in position of the Light Sensor. The uncertainty in distance between the projection surface and the slits would also improve upon a more precise method by implementation of a Rotatory Motion Sensor.

Furthermore, follow-up experiments have been proposed in Section 4.2. A number of variables have not been altered. The effect of different wavelengths, aperture sizes or additional slits on the interference pattern could help in understanding the wave behaviour further. One could also replicate the experiment with other types of waves, documenting the similarities. The range of possibilities is wide, as the experiment has been fundamental to the development and understanding of modern physics for a reason.

References

[1] 'May 1801: Thomas Young and the Nature of Light', American Physical Society, 2024. [Online]. Available: https://www.aps.org/archives/publications/apsnews/200805/physicshistory.cfm.

[2] T. Commissariat, 'Two paths, diverged', *Phys. World*, vol. 31, no. 9, pp. 44–45, Sep. 2018.

[3] J. F. Schonfeld, 'Analysis of Double-slit Interference Experiment at the Atomic Level', *Studies in History and Philosophy of Science Part B: Studies in History and Philosophy of Modern Physics*, 2019. [Online]. Available: https://api.semanticscholar.org/CorpusID:141365029.

[4] E. T. H. Wu, 'Time, space, gravity and spacetime based on yangton & yington theory, and spacetime shrinkage versus universe expansion', en, *Am. J. Mod. Phys.*, vol. 5, no. 4, p. 58, 2016.

[5] *Interference and Diffraction of Light Experiment EX-5545A*, PASCO scientific, 2024. [Online]. Available: https://www.pasco.com/products/complete-experiments/waves-and-optics/interference-and-diffraction-of-light-experiment.

[6] J. Yee, 'Photon Creation and Absorption', in *The Particles of the Universe*, Independently published, 2012, ISBN: 978-1731583734. [Online]. Available: https://energywavetheory.com/photons/photon-interactions/.

[7] K. Stamnes, 'Ultraviolet Radiation', in *Encyclopedia of Atmospheric Sciences*, J. R. Holton, Ed., Oxford: Academic Press, 2003, pp. 2467–2473, ISBN: 978-0-12-227090-1. DOI: https://doi.org/10.1016/B0-12-227090-8/00444-9. [Online]. Available: https://www.sciencedirect.com/science/article/pii/B0122270908004449.

[8] S. J. Ling, J. Sanny and W. Moebs, *University Physics III: Optics and Modern Physics (OpenStax)*, en. OpenStax, Sep. 2016.

[9] P. P. Urone and R. Hinrichs, *College Physics 2e*, en. OpenStax, 2022.

[10] GeeksforGeeks. 'Single Slit Diffraction: Definition, Formula, Types and Examples'. (2023), [Online]. Available: https://www.geeksforgeeks.org/single-slit-diffraction/ (visited on 19/11/2024).

[11] L. coordinators et. al, *O1 – Interference and Diffraction of Light*, 2024.